

DALHOUSIE UNIVERSITY

A QUANTITATIVE ANALYSIS OF DEGLACIATION  
AS A POSSIBLE EARTHQUAKE MECHANISM  
IN CANADA

SUBMITTED TO  
THE DEPARTMENT OF GEOLOGY  
IN CANDIDACY FOR THE DEGREE OF  
BACHELOR OF SCIENCE

BY  
ALLISON L. BENT

HALIFAX, NOVA SCOTIA

MARCH 1985



DALHOUSIE UNIVERSITY

Department of Geology

Halifax, N.S. Canada B3H 3J5

Telephone (902) 424-2358 Telex: 019-21863

DALHOUSIE UNIVERSITY, DEPARTMENT OF GEOLOGY

B.Sc. HONOURS THESIS

Author: Allison L. Bent

Title: A Quantitative Analysis of Deglaciation  
as a Possible Earthquake Mechanism in Canada

Permission is herewith granted to the Department of Geology, Dalhousie University to circulate and have copied for non-commercial purposes, at its discretion, the above title at the request of individuals or institutions. The quotation of data or conclusions in this thesis within 5 years of the date of completion is prohibited without permission of the Department of Geology, Dalhousie University, or the author.

The author reserves other publication rights, and neither the thesis nor extensive extracts from it may be printed or otherwise reproduced without the authors written permission.

Signature of author

Date: 03.04.85

COPYRIGHT

## Distribution License

DalSpace requires agreement to this non-exclusive distribution license before your item can appear on DalSpace.

### NON-EXCLUSIVE DISTRIBUTION LICENSE

You (the author(s) or copyright owner) grant to Dalhousie University the non-exclusive right to reproduce and distribute your submission worldwide in any medium.

You agree that Dalhousie University may, without changing the content, reformat the submission for the purpose of preservation.

You also agree that Dalhousie University may keep more than one copy of this submission for purposes of security, back-up and preservation.

You agree that the submission is your original work, and that you have the right to grant the rights contained in this license. You also agree that your submission does not, to the best of your knowledge, infringe upon anyone's copyright.

If the submission contains material for which you do not hold copyright, you agree that you have obtained the unrestricted permission of the copyright owner to grant Dalhousie University the rights required by this license, and that such third-party owned material is clearly identified and acknowledged within the text or content of the submission.

If the submission is based upon work that has been sponsored or supported by an agency or organization other than Dalhousie University, you assert that you have fulfilled any right of review or other obligations required by such contract or agreement.

Dalhousie University will clearly identify your name(s) as the author(s) or owner(s) of the submission, and will not make any alteration to the content of the files that you have submitted.

If you have questions regarding this license please contact the repository manager at [dalspace@dal.ca](mailto:dalspace@dal.ca).

Grant the distribution license by signing and dating below.

---

Name of signatory

---

Date

TABLE OF CONTENTS

ILLUSTRATIONS.....ii

ABSTRACT.....iii

Chapter

I. INTRODUCTION.....1

II. RESPONSE TO LOADING.....6

    Viscous Response.....6

    Elastic Response.....10

    Brittle Response.....13

III. OBSERVED SEISMICITY.....16

IV. ICE MODEL.....21

V. RESULTS AND DISCUSSION.....27

VI. CONCLUSIONS.....30

REFERENCES.....31

APPENDIX 1.....34

APPENDIX 2.....35

APPENDIX 3.....40

## ILLUSTRATIONS

### Figure

1. Canadian Earthquakes .....	4
2. Stresses Induced by Deglaciation.....	5
3. Relations Between Different Magnitudes.....	17
4. Green's Function.....	22
5. Laurentide Ice Sheet at 18000BP.....	24
6. Laurentide Ice Sheet at 10000BP.....	24

### Map

1. Observed Seismicity
2. Theoretical Seismicity

## ABSTRACT

With the exception of earthquakes occurring along the Pacific coast, earthquakes in Canada cannot be explained by plate tectonic theory. Deglaciation has been proposed as a possible cause of non-tectonic Canadian earthquakes.

The main objective of this study was to determine, through the use of computer models, whether earthquakes in Canada are caused by post-glacial uplift. The observed seismic moment densities in all parts of Canada were determined from the magnitudes of about 10000 earthquakes occurring over a 400 year time interval. The theoretical seismic moment densities were calculated from the strain rates associated with the retreat of the Laurentide ice sheet. The model used to approximate the removal of the ice sheet was based on the work of Peltier and Andrews (1976).

Contour maps of both the theoretical and observed seismic moment densities were made in order to compare the magnitude and distribution of actual and predicted seismicity. Although the distribution patterns differ somewhat, in all areas the predicted seismicity due to deglaciation is sufficient to account for the observed seismicity.

## INTRODUCTION

Earthquakes generally occur at the boundaries of lithospheric plates where one plate is moving relative to another. Canada, with the exception of the Pacific coast, is an intraplate region and should therefore be earthquake-free according to plate tectonic theory. A large number of earthquakes, however, have occurred in Canada (figure 1) in areas where their occurrences cannot be explained by plate tectonics.

There are several possible non-tectonic earthquake mechanisms. In areas which were once covered by glacial ice, which includes most of Canada, deglaciation is a possible cause of earthquakes. As the ice melted, the downward pressure on the continents decreased causing extension, while the increased mass in the oceans caused compression of the oceanic crust (figure 2). Because the earth as a whole behaves viscoelastically and does not readjust instantaneously to the redistribution of mass, but re-establishes equilibrium over a period of time, the strain rates associated with post-glacial rebound can be determined and compared to the strain rates due to seismic slip in order to determine whether there is any similarity between them.

Similarly, in areas along continental margins, sediment loading may be the cause of earthquakes. Removal of

sediment from the continents and subsequent deposition on the continental shelves results in extension and compression of the continent and ocean respectively.

The earth is not a perfect sphere. The lithospheric plates must therefore change their shapes as they move from one area to another. This process results in membrane stresses throughout the plates which may cause earthquakes. Another possibility is regional stress caused by the transmission of tectonic forces from the plate boundary through the plate.

Gravity anomalies provide information about the state of stress of the lithosphere and may, therefore, provide information about the origin of earthquakes. Since gravitational force is proportional to mass and stress is proportional to force, gravitational measurements should reveal whether the stresses in a given area are caused by an excess or a deficiency of mass.

I have studied only deglaciation as a possible earthquake mechanism in Canada. To determine whether this process is significant in earthquake generation, the theoretical and observed values of seismic strain release were calculated in terms of seismic moment and compared. The observed values were determined from the magnitudes and epicentres of recorded Canadian earthquakes using the relation between magnitude and seismic moment. Computer models were developed to determine the theoretical seismicity due to deglaciation and were based on the relationships between uplift velocity, strain rate and



seismic moment, the first of which was determined from the rate of deglaciation.

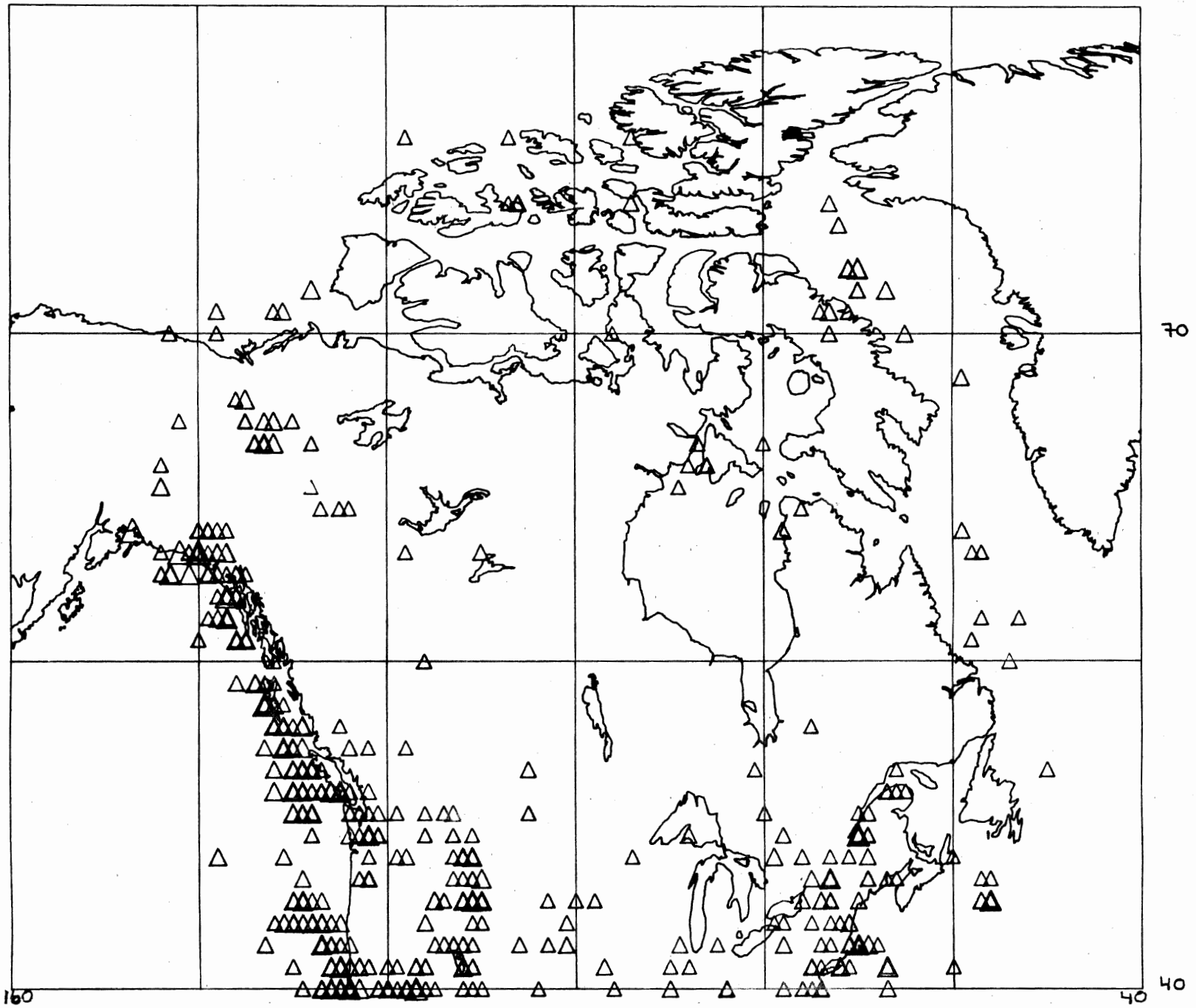


Fig.1.Epicentres of Canadian earthquakes,1568-1981,with  $M \geq 5$ .

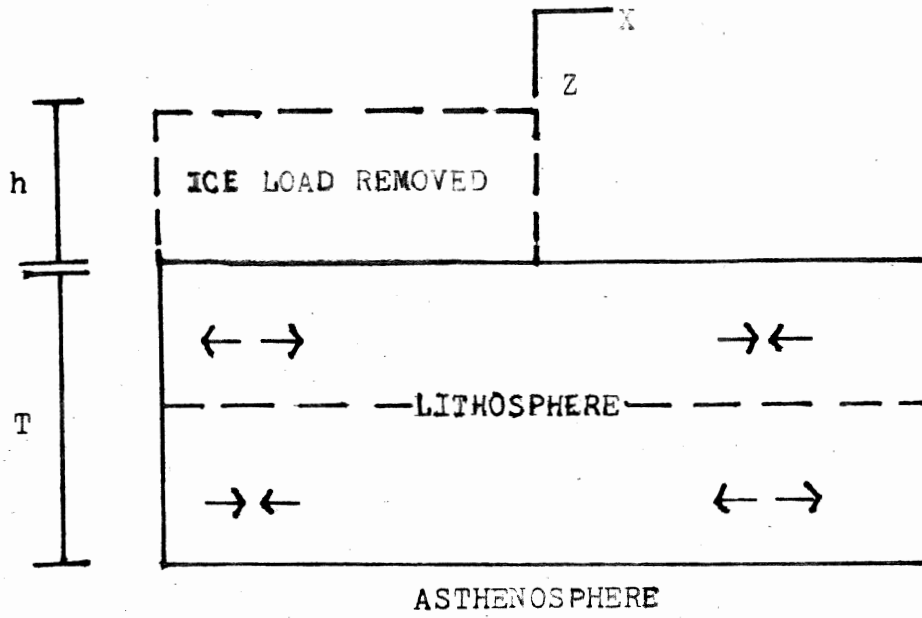


Fig.2. Orientation of stresses induced by deglaciation. The dashed line in the lithosphere represents the neutral plane (after Stein et al., 1979).

## RESPONSE TO LOADING

### Viscous Response

Although the earth as a whole behaves viscoelastically, it is actually composed of several distinct regions which behave differently. The earth's structure can be described by three layers consisting of a lower viscous half-space, which flows in response to stress, a middle elastic layer, which bends under stress, and an upper brittle layer which fractures under stress. The time history of flexure due to a point load is calculated for each layer beginning with the viscous half-space.

It is assumed that at a time in the past,  $t=0$ , the earth was in isostatic equilibrium. For all calculations, time is measured in terms of this time which corresponds to the beginning of the retreat of the Laurentide ice sheet. Vertical distances,  $z$ , are positive downward and are measured with respect to the neutral plane—the plane which does not change its dimensions under deformation.

For the asthenosphere, the equations for an incompressible viscous fluid are used. The Navier-Stokes equation relates accelerational and viscous forces:

$$\rho \ddot{u} = -\nabla p + \eta \nabla^2 u = 0 \quad |$$

(Wu&Peltier,1982) where  $\rho$  is the density of the asthenosphere,  $\eta$  is the viscosity,  $p$  is the pressure  $p(x,y,z)$  due to a point load,  $\underline{u}$  is the velocity  $\underline{u}(u,v,w)$  where  $u,v$ , and  $w$  are the velocities in the  $x,y$ , and  $z$  directions respectively, and  $\dot{\underline{u}}$  is the time derivative of  $\underline{u}$ . The Navier-Stokes equation is equal to zero since the rate of flow in the asthenosphere is extremely slow. An harmonic load is assumed initially so that

$$p=P(z)e^{i(kx+ly)}$$

$$u=U(z)e^{i(kx+ly)}$$

$$v=V(z)e^{i(kx+ly)}$$

$$w=W(z)e^{i(kx+ly)}$$

$$f=F(z)e^{i(kx+ly)}$$

where  $f(x,y,z)$  is the stress caused by the load, and  $k$  and  $l$  are wave numbers. At  $z=0$ , the stress is equal to the pressure, which is defined as

$$p(x,y,0)=P(0)e^{i(kx+ly)}$$

From the  $z$ -component of equation 1, it can be seen that

$$\nabla^2 w = P' e^{i(kx+ly)}$$

Therefore

$$\begin{aligned} P'e^{i(kx+ly)} &= \eta (-k^2 W e^{i(kx+ly)} - l^2 W e^{i(kx+ly)} + W'' e^{i(kx+ly)}) \\ &= \eta (-(k^2+l^2) W e^{i(kx+ly)} + W'' e^{i(kx+ly)}) \end{aligned}$$

and

$$P' = \eta (-K^2 W + W'') \quad 2$$

where  $K^2$  is defined as  $k^2+l^2$ . The 0-value of the x-component of equation 1 requires that

$$\partial p / \partial x = \eta \nabla^2 u = ik P e^{i(kx+ly)}$$

Solving as for  $P'$ , the following result is obtained:

$$ikP = \eta (-k^2 U + U'') \quad 3$$

Similarly,

$$ilP = \eta (-l^2 V + V'') \quad 4$$

Differentiating equations 2, 3, and 4 with respect to

z, x, and y respectively results in

$$\begin{aligned}\eta(-K^2W'+W''') &= P' & 5 \\ \eta(-kU'+ikU''') &= -k^2P & 6 \\ \eta(-lV'+ilV''') &= -l^2P & 7\end{aligned}$$

The sum of equations 5, 6, and 7 gives the result

$$\nabla \cdot \underline{u} = P'' - K^2P$$

Since the velocity divergence is 0 due to incompressibility (Wu & Peltier, 1982)

$$P'' - K^2P = 0 \quad 8$$

The differential equation 8 is solved for pressure so that

$$P(z) = P_0 e^{-Kz}$$

if K is less than zero, and since P approaches 0 as z becomes infinitely large,

$$P(z) = P_0 e^{-|K|z}$$

if  $k$  is greater than 0.

Therefore,

$$\begin{aligned} W'' - K^2 W &= P' / \\ &= -KP_0 e^{-|K|z/\eta} \end{aligned} \quad 9$$

Since  $U(0)=V(0)=0$ , the exact solution of the differential equation 9 can be obtained. The vertical velocity,  $W$ , is

$$W = P_0 / 2\eta \cdot (z + K^{-1}) e^{-|K|z} \quad 10$$

#### Elastic Response

For the elastic layer,  $w$  denotes the vertical displacement and not the velocity as it did for the viscous medium. The formula for the bending of a thin elastic plate is applied:

$$f(u) - \rho g w - P_\eta = N \nabla^2 (\nabla^2 w) \quad 11$$

(Wu & Peltier, 1982) where  $g$  is the acceleration due to gravity,  $P_\eta$  is the pressure due to the viscous layer and  $N$



is the flexural rigidity. As for the asthenosphere, the load is assumed to be harmonic. It follows from equation 10 that

$$P(0) = 2K\eta \dot{w} \quad 12$$

where  $\dot{w}$  is the velocity  $\partial w / \partial t$ .

Equation 12 is then substituted into equation 11 so that

$$NK^4 w = F - \rho g w - 2|K|\dot{w}\eta \quad 13$$

Solving equation 13 for vertical displacement yields the following result:

$$w = F / (NK^4 + \rho g) \cdot (1 - \exp(-(NK^4 + \rho g)t / 2\eta |K|))$$

where the exponential term represents the response to the load and the relaxation time is  $((NK^4 + \rho g) / 2\eta |K|)^{-1}$ .

The impulse response to a unit load at the origin is the Green's function:

$$G(x, y) = 1 / ((2\pi)^2) \int_{-\infty}^{\infty} \int_{-\infty}^{\infty} (NK^4 + \rho g) x (1 - \exp(-(NK^4 + \rho g)t / 2\eta |K|)) e^{i(kx + ly)} dk dl$$

Two substitutions are made:

$$A(K) = 1 / ((2\pi)^2 (NK^4 + \epsilon g)) \cdot (1 - \exp(-(NK^4 + \epsilon g)t / 2\eta |K|))$$

and

$$\underline{K} \cdot \underline{r} = K r \cos \theta = kx + ly$$

so that

$$G(r, \theta) = \int_0^{\infty} A(K) \int_0^{2\pi} e^{iKrcos\theta} K d\theta dK \quad 14$$

Using the Bessel function of the first order:

$$J_0(Kr) = 1/2\pi \int_0^{2\pi} e^{iKrcos\theta} d\theta$$

equation 14 can be expressed as a Hankel transform of A(K) and therefore

$$G(r) = 2\pi \int_0^{\infty} A(K) J_0(Kr) dK$$

Resubstituting the original values into the above equation results in

$$G(r) = 1/2\pi \int_0^{\infty} 1/(NK^4 + e g) \cdot (1 - \exp(-(NK^4 + e g)t/2\eta K)) J_0(Kr) dK \quad 15$$

By differentiating equation 15 with respect to time, the Green's function for velocity is obtained:

$$\dot{G}(r,t) = 1/4\pi\eta \int_0^{\infty} \exp(-(NK^4 + e g)t/2\eta K) J_0(Kr) dK \quad . \quad 16$$

### Brittle Response

It is assumed that all earthquakes occur in the brittle layer, which responds to stress only by fracturing. The total displacement along a fault is related to the dislocation of the elastic layer. The average displacement along a fault is related to the seismic moment by the equation

$$M_0 = \mu A \bar{u} \quad 17$$

(Brune, 1968; Maruyama, 1963; Haskell, 1963; Burridge & Knopoff, 1964; Aki, 1966) where  $M_0$  is the seismic moment,  $\mu$  is the rigidity,  $A$  is the area of the fault plane, and  $\bar{u}$  is the average dislocation along the fault plane. For large earthquakes the seismic moment is related

to the surface- wave magnitude(Kanamori&Anderson,1975) by

$$\log_{10}M_0=1.5M_S+8.5$$

18

If an elastic plate is bent by an extensional force, extension occurs above the neutral plane and compression below. In seismicity determinations, only the section above the neutral plane is significant since no earthquakes occur below it. The lack of earthquakes below the neutral plane is probably due to the temperature, which is high enough for the rocks to deform plastically.

The strain in a plane of infinitesimal thickness is

$$e = \partial u / \partial x = \kappa \cdot z$$

19

where  $e$  is the strain and  $\kappa$  is the curvature  $\partial^2 w / \partial x^2$ .

For the purposes of calculations, it is assumed that all deformation of the brittle layer occurs along a single fault. This assumption is valid since for a specific strain value, the total displacement in a volume is constant whether it occurs along a single fault or several smaller ones.

The horizontal displacement along the fault plane is  $U$ , the dip of the fault plane is  $\Theta$ ,  $W$  is the width,  $h$  is the thickness, and  $X$  is the total length perpendicular to the width. The net displacement along the fault plane is

defined as

$$u=U/\cos \theta$$

and the area of the fault is

$$A=Wh/\sin \theta$$

Thus

$$Au=UWh/\cos \theta \sin \theta$$

Equation 20 is minimized by assuming the ideal situation, that is that the dip is  $45^\circ$ , resulting in

$$Au=2UV/X$$

20

where V is volume.

Using the results of equations 17 and 19, the seismic moment can be determined by

$$M_0=2\mu eV$$

## OBSERVED SEISMICITY

The epicentres, magnitudes and times of all recorded Canadian earthquakes from 1568 to 1977 were transferred from an Earth Physics Branch data tape to a computer file. The same information for earthquakes of magnitude 3 and higher occurring from 1978 to 1981 (Energy, Mines and Resources Canada. Earth Physics Branch, 1979, 1980, 1981, 1984) was added to the file. Data from 1982 to the present and before 1568 were not available. The distribution of earthquakes of magnitude 5 and higher is shown in figure 1.

Surface-wave magnitudes were not recorded for all earthquakes. Since the moment-magnitude relation (equation 18) requires surface-wave magnitudes, it was necessary to determine empirical relations between the surface-wave magnitude and each of body-wave magnitude ( $M_B$ ), local magnitude ( $M_L$ ), and Nuttli magnitude ( $M_N$ ). The relations were obtained by plotting each of the other magnitudes against the surface-wave magnitude of those earthquakes for which both magnitudes were recorded. The results are shown in figure 3 and are as follows:

$$M_S = -5.2 + 2.0M_B$$

$$M_S = 1.2 + 0.5M_L$$

$$M_S = -4.2 + 1.8M_N$$

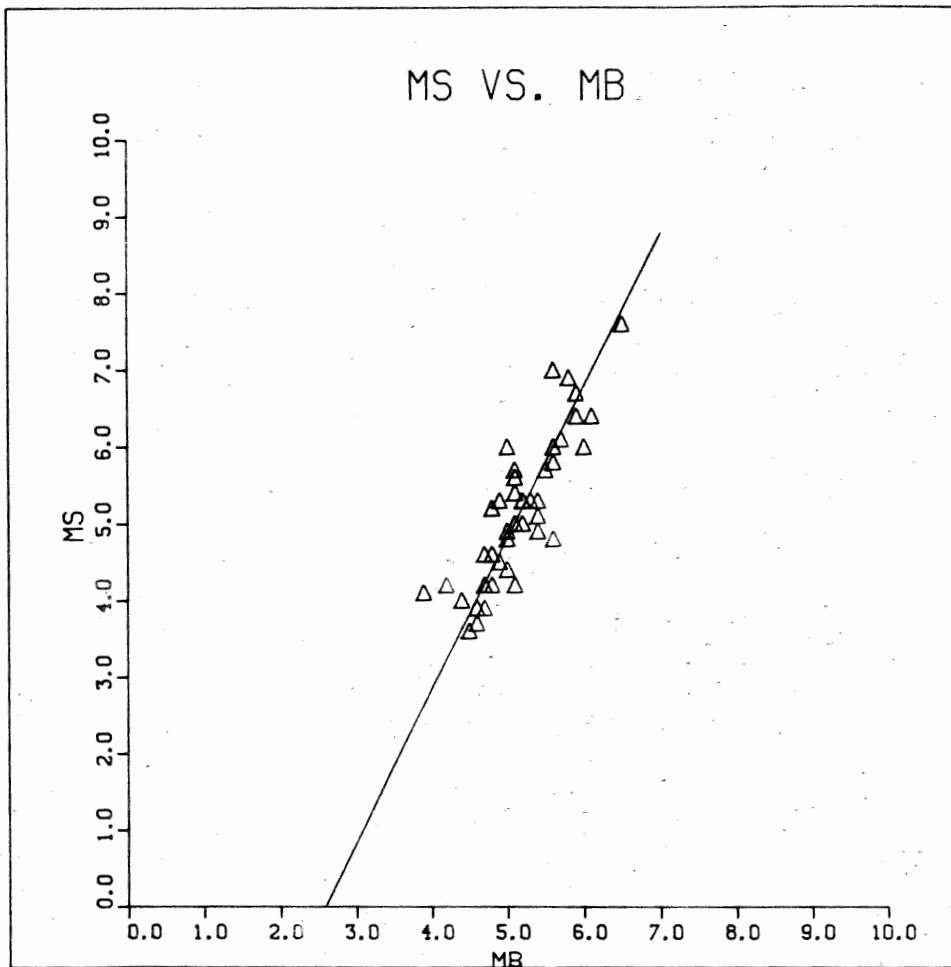


Fig.3a. The relation between surface-wave and body-wave magnitudes.

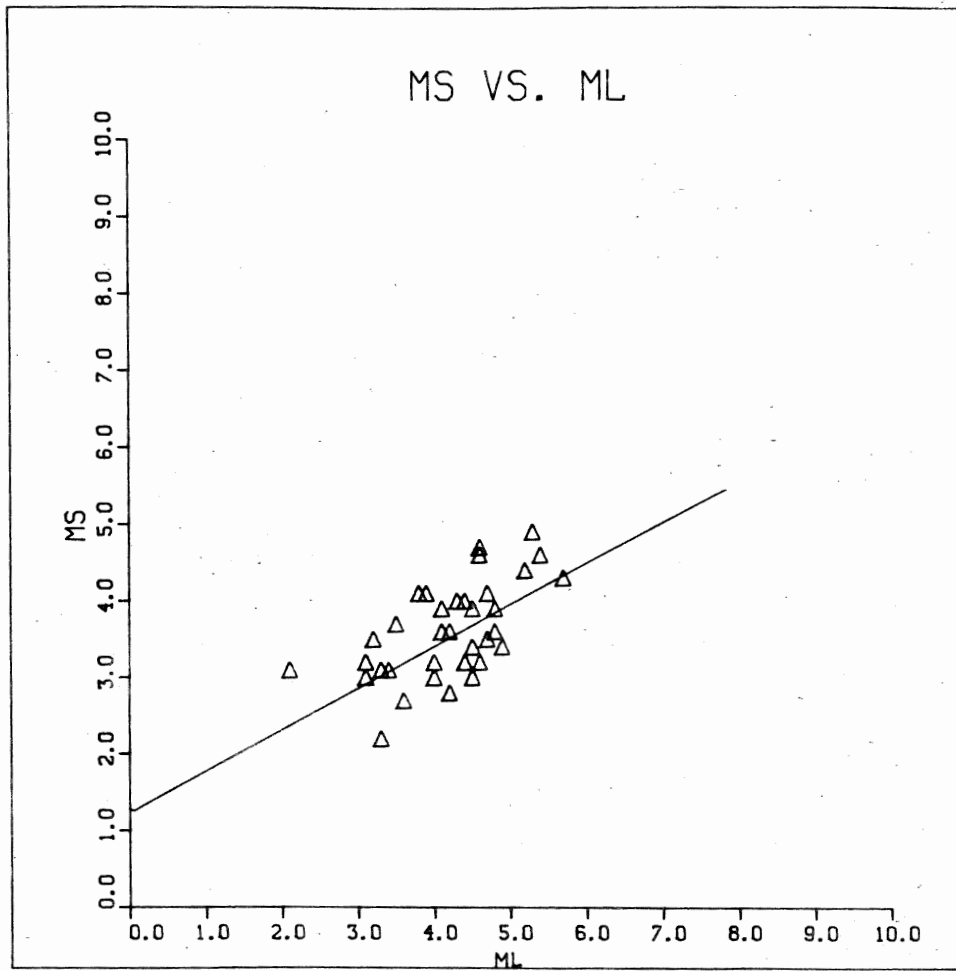


Fig.3b. The relation between surface-wave and local magnitudes.



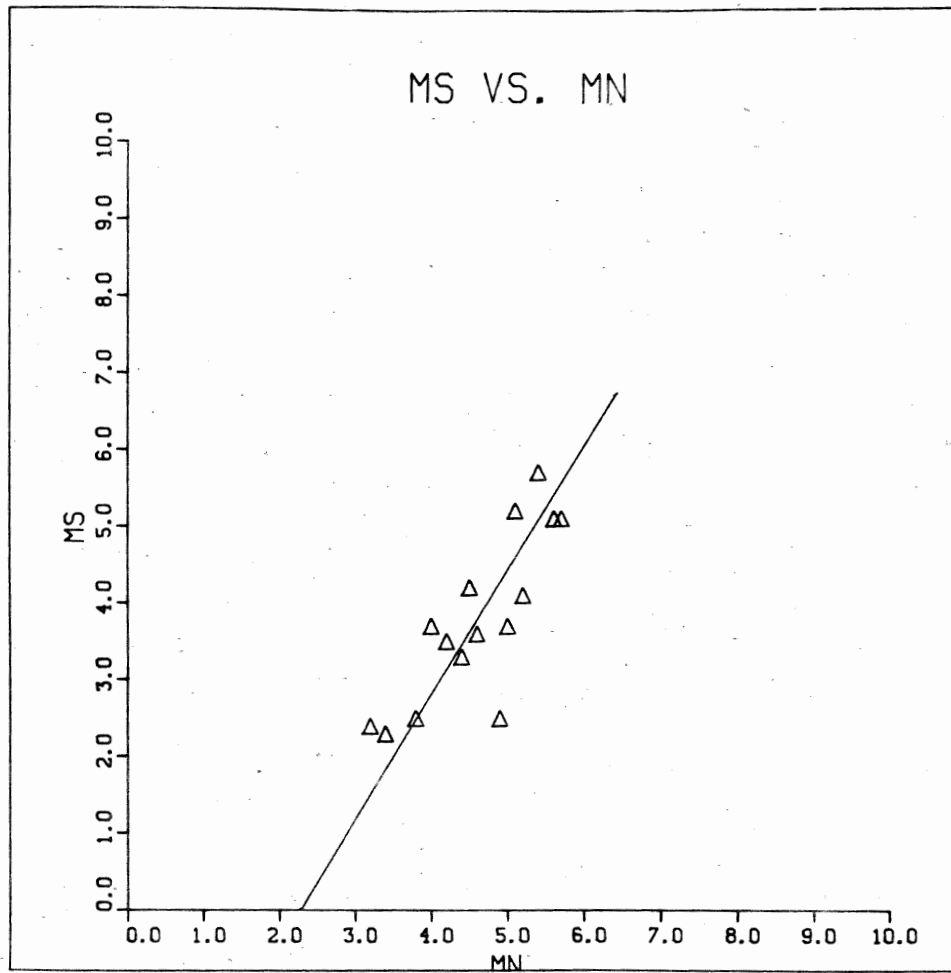


Fig.3c. The relation between surface-wave and Nuttli magnitudes.

These equations hold true only for Canadian earthquakes and may not be true for extremely large or extremely small earthquakes.

The region from  $40^{\circ}\text{N}$  to  $85^{\circ}\text{N}$  and  $40^{\circ}\text{W}$  to  $160^{\circ}\text{W}$  was divided into blocks measuring  $5^{\circ}$  by  $5^{\circ}$ . Using equation 18, the total seismic moment for each block was calculated. Surface-wave magnitude was used when available otherwise the recorded magnitude was converted to surface-wave magnitude by the appropriate conversion equation. The seismic moment densities were determined by dividing the total magnitude of the block by the area of the block and by 400 years—the approximate length of the earthquake record. The results were then multiplied by a conversion factor so that the moment density units were  $\text{N}\cdot\text{m}/\text{m}^2\cdot\text{yr}$ . The seismic moment densities were plotted and contoured. The results are shown in map 1.

## ICE MODEL

Using equation 15, the Green's velocity functions were calculated for various times and distances. The times used were 16000, 13000, 11000, 9000, and 7000 years before the present. For each of these times, the Green's function was calculated at 100km intervals from 0km to 2000km. In calculating the Green's functions, the values of Stein et al (1979) were used:  $\eta = 10^{21} \text{Pa} \cdot \text{s}$ ,  $\rho = 3300 \text{kg m}^{-3}$ ,  $g = 9.8 \text{m} \cdot \text{s}^{-2}$ .  $N$  was calculated using the equation

$$N = ET^3 / 12(1 - \sigma^2)$$

where the Young's Modulus,  $E$ , is  $6.5 \times 10^{10} \text{N m}^{-2}$ , Poisson's ratio,  $\sigma$ , is 0.25, and the lithospheric thickness,  $T$ , is  $100 \times 10^3 \text{m}$ . The Green's function values were obtained by numerical integration using the trapezoidal rule. Intervals  $dK$  of  $10^{-8}$  were used for values of  $K$  from 0 to 0.001 or from 0 until the exponential term was less than  $e^{-50}$ . For larger values of  $K$ , the response is negligible and was therefore ignored. The results are listed in Appendix 1 and the variation of the Green's function with distance at 16000BP is shown in figure 4.

The rate of uplift was obtained by convolving the Green's functions with the ice load. The ice distribution and

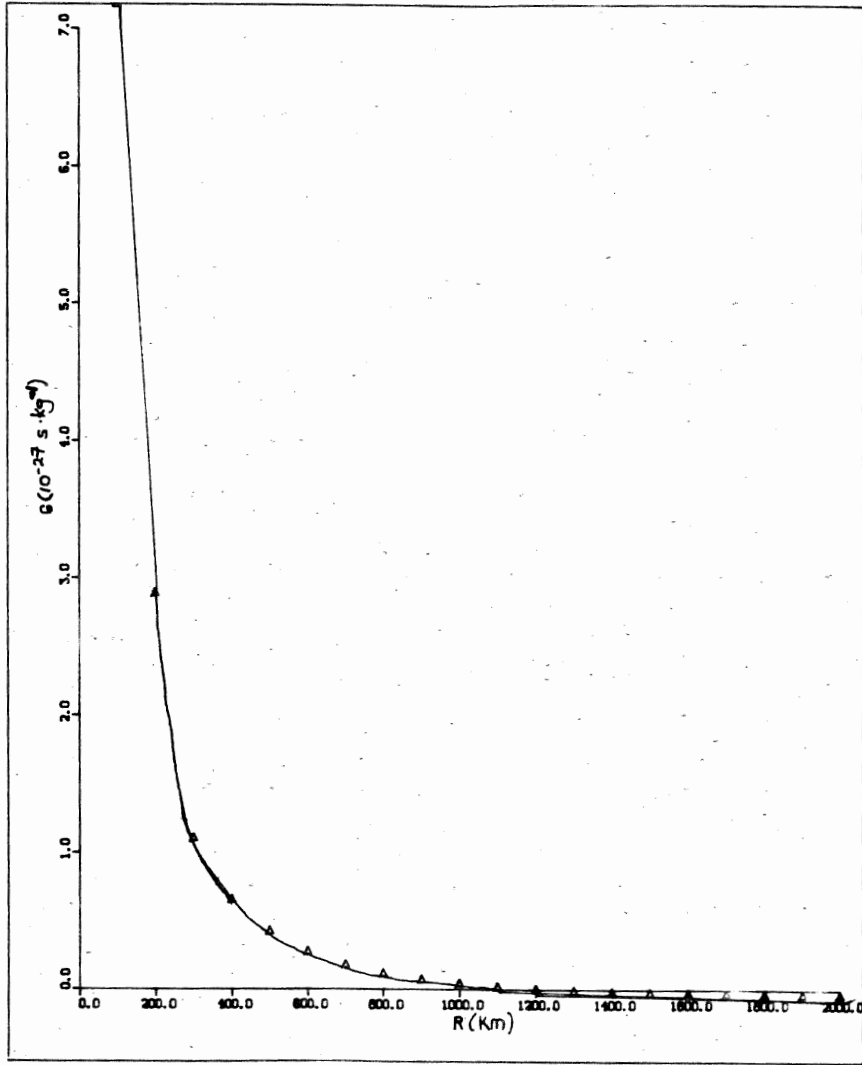


Fig.4.Variation of Green's(velocity) function with distance at 16000BP.

thickness at 18000BP and 10000BP are shown in figures 5 and 6. The actual values(Appendix 2) used were those of Peltier and Andrews (1976),which were obtained through a model of isostatic adjustment.

Peltier and Andrews(1976) assumed that at 18000BP(the time of the maximum Wisconsin glaciation)the earth was a perfect sphere in a state of isostatic equilibrium and that the redistribution of mass associated with deglaciation upset the gravitational equilibrium and caused the earth to change its shape,although not significantly. They also assumed that the readjustment occurred both elastically and anelastically. The time history of the change in local radii was determined from relative sea level curves,which were obtained from radiometric dating of objects whose presence or absence depends on the distance from the ice sheet,and by calculating the change in ice thickness required to produce the calculated sea level changes.

For the seismicity determinations,I approximated the continuous changes in ice thickness by assuming that the ice was removed in discrete units,and used removal times to correspond to the times for which ice thickness data were available

(Peltier and Andrews,1976):18000,14000,12000,10000,8000,and 6000 years before the present,and assumed that no ice was removed after 6000BP. To determine the rate of uplift of the lithosphere,the Green's function was obtained by using a computer program which modified it from that of a point load to that of a cone with a radius of  $1^{\circ}$  latitude in order to

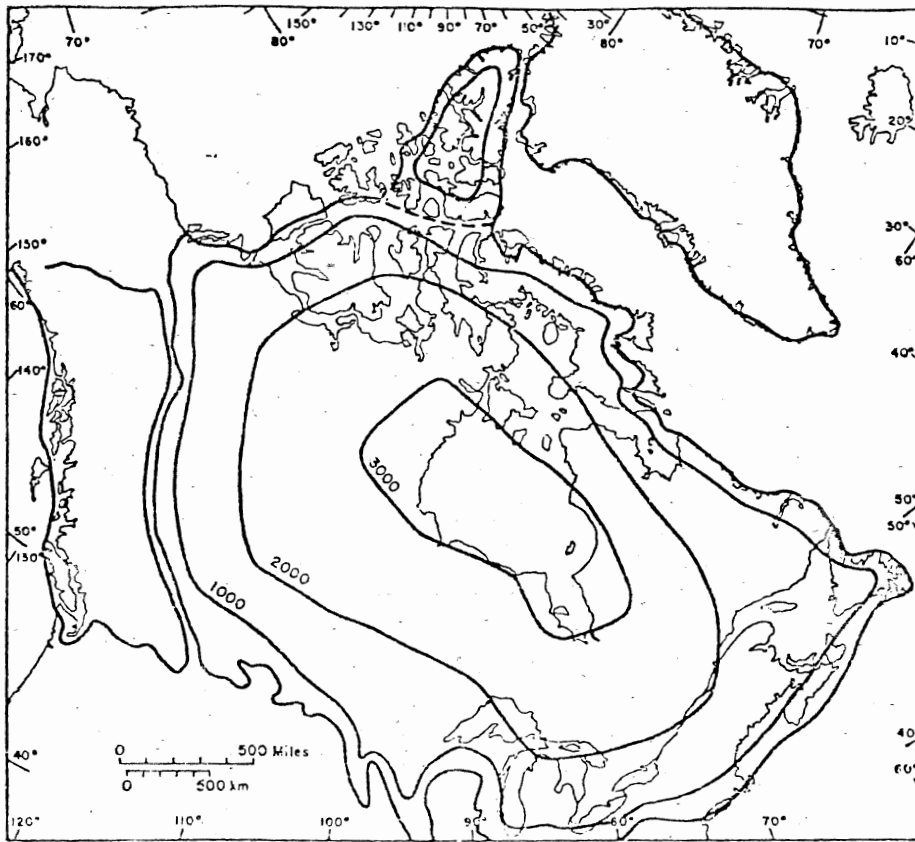


Fig.5. Laurentide ice thickness at 18000BP  
(from Peltier&Andrews,1976).

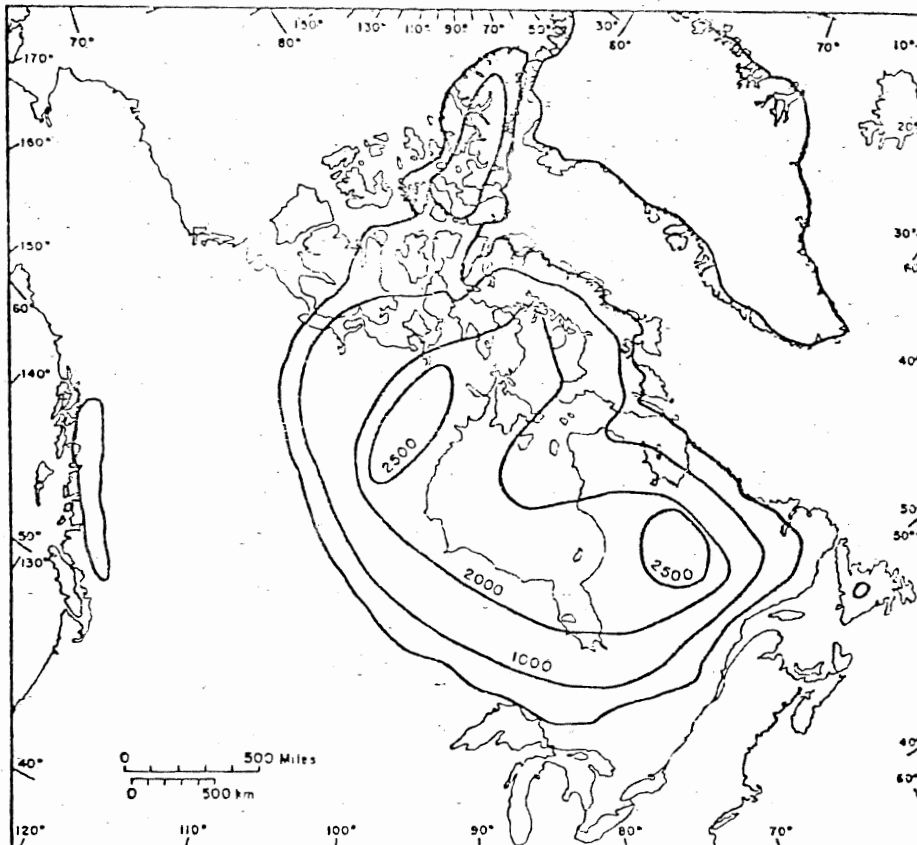


Fig.6 Laurentide ice thickness at 10000BP  
(from Peltier&Andrews,1976).

obtain a better approximation of the actual ice load. The velocity is

$$\dot{w} = \sum_{r=0}^{2 \times 10^3} \sum_{t=0}^{12 \times 10^3} \dot{G}(r, \bar{t}) \Delta h_{t1, t2} \rho_i g \delta A$$

where  $\Delta h$  is the height of the ice column removed between times  $t_1$  and  $t_2$ ,  $\rho_i$ , the ice density, is  $1000 \text{ kg m}^{-3}$ ,  $\delta A$  is the increment of area and  $\bar{t}$  is the mean of  $t_1$  and  $t_2$ . The velocity was calculated at points every  $1^\circ$  latitude and every  $2.5^\circ$  longitude, assuming that the ice thickness varied linearly between the points for which data were available.

By taking the time derivative of equation 19, the strain rates are

$$\begin{aligned} \dot{e}_{xx} &= z \partial^2 w / \partial x^2 \\ \dot{e}_{yy} &= z \partial^2 w / \partial y^2 \\ \dot{e}_{xy} &= z \partial^2 w / \partial x \partial y \end{aligned}$$

The velocity gradients were calculated over distances  $dx=2.5^\circ$  longitude and  $dy=1^\circ$  latitude. The strain rates were determined at points every  $5^\circ$  latitude and longitude. The strain  $e_{xy}$  does not have an effect on the compression of the lithosphere so it was necessary to shift the x- and y-axes so that the strain rate  $\dot{e}'_{xy}=0$ . The modified strain rates are

$$\dot{e}_{xx}' = ((\dot{e}_{xx} + \dot{e}_{yy})/2) + ((\dot{e}_{xx} - \dot{e}_{yy})^2/2 + \dot{e}_{xy}^2)^{1/2}$$

$$\dot{e}_{yy}' = ((\dot{e}_{xx} + \dot{e}_{yy})/2) - ((\dot{e}_{xx} - \dot{e}_{yy})^2/2 + \dot{e}_{xy}^2)^{1/2}$$

The strain is plane strain so the total strain rate in the x'y'-plane is the sum of the magnitudes of the individual strain rates:

$$\dot{e} = |\dot{e}_{xx}'| + |\dot{e}_{yy}'|$$

It follows from equation 21 that

$$M_0/At = 2\mu \int_0^z \dot{e}(z) z dz \quad 22$$

where  $\mu = 3.3 \times 10^{10} \text{ N} \cdot \text{m}^{-2}$  and  $z = 50 \times 10^3 \text{ m}$ . The moment densities were calculated for points every  $5^\circ$  latitude and longitude and were then plotted and contoured. The results are shown in map 2.



## RESULTS AND DISCUSSION

A comparison of the observed seismic moment densities (map 1) with the theoretical moment densities due to deglaciation (map 2) reveals that the theoretical moment densities are several orders of magnitude greater than the observed values. The average theoretical moment density is of the order of  $10^7$ . The observed values range from  $10^{-13}$  to  $10^0$  and there are also some areas of 0 seismicity.

There are several explanations for the differences between the observed and theoretical seismic moment densities. The observed seismicity is probably less than the true seismicity because the seismic record, particularly in the north, is very short and incomplete. Earthquakes of the same magnitudes as those observed, however, would not increase the seismicity to that predicted by the ice model unless a large number of moderate to large earthquakes were not recorded. For example, one magnitude 6 earthquake in  $5^\circ$  by  $5^\circ$  block at  $50^\circ\text{N}$  during a 400 year interval would increase the seismic moment density by a number of the order of  $10^{-4}\text{N}\cdot\text{m}/\text{m}^2\text{yr}$ . Therefore unless earthquakes of magnitude 7-8 occurred but were unnoticed or occur in the future in all regions (except the west coast), the differences between the observed and theoretical seismic moment densities are probably caused by assumptions made in the ice model.

It was assumed that earthquakes could occur at any

depth in the brittle layer. In reality, Canadian earthquakes tend to be shallow and rarely occur below 30km. Changing the lower limit of the integral in equation 22 from 0 to 30km would decrease the theoretical value although not significantly.

Another assumption was that the brittle layer responds to stress only by fracturing. It is more probable that the layer responds by partially elastic and partially brittle behavior. Even if the layer exhibits greater than 99% elastic behavior, there will be sufficient strain release by fracturing to explain the occurrence of earthquakes.

The deglaciation model predicts a fairly uniform seismic moment density whereas the observed distribution pattern is much more complex. There are two probable reasons for this discrepancy. The theoretical seismic moment density calculations ignored regional variations in the strength of the lithosphere. Several of the areas where the seismicity is high, such as the St. Lawrence Valley and Baffin Bay, are thought to be located on ancient failed rifts. Thus, the crust is weaker in these regions, requires less stress to fracture and is, therefore, more active. Areas of high seismicity also tend to be near the coast. If sediment loading as well as deglaciation can generate earthquakes, then the combined strain rates would be highest in coastal areas while further inland, the strain release would be due to deglaciation only and, therefore, probably less. The resulting seismic moment densities would then show more regional variation. The strain release due to

sediment loading is not presently available to test this hypothesis.

Stresses were not calculated in this study, but stress as well as strain rate is important in earthquake generation. Although the strain rates associated with deglaciation are large, the stresses are not. Past work (Stein et al, 1979; Quinlan, 1984) has shown that the stresses associated with deglaciation are sufficient to fracture previously weakened crust. If deglaciation is the cause of earthquakes, then due to the orientation of the resulting stresses, normal faulting should occur on land and reverse faulting in the offshore areas. These fault mechanisms are observed (Stein et al, 1979; Quinlan, 1984), but these studies, which included only a limited number of earthquakes, reached opposite conclusions with respect to the reliability of the orientations of the calculated stresses and whether they can be used to determine the type of failure. If the ambient stresses, however, are just below those required for fracture, then the combined effect of ambient and load stresses should be sufficient to explain the observed seismicity. A comparison of the total stress drop due to earthquake activity and the total stress (background plus deglaciation-induced) would reveal whether that, in fact, is true.

## CONCLUSIONS

The strain release associated with deglaciation is more than sufficient to generate non-tectonic earthquakes. An incomplete earthquake record and assumptions made in the ice model are the most likely causes of the differences between the observed and theoretical seismic moment densities. Further work comparing observed and theoretical stress drops would be useful in refining the model and explaining regional variations in seismicity, as would the determination of the strain rates due to sediment loading. Nevertheless, the evidence strongly implies that deglaciation is the cause of non-tectonic earthquakes in Canada. Based on strain rates, the potential for large earthquakes exists in all regions of Canada.

## REFERENCES

Aki, K., "Generation and propagation of G waves from the Niigata earthquake of June 16, 1964, 2, Estimation of earthquake moment, released energy, and stress-strain drop from the G wave spectrum", Bulletin of Earthquake Research Institute Tokyo University, 44, 73, 1966.

Brune, J.N., "Seismic moment, seismicity, and rate of slip along major fault zones", Journal of Geophysical Research, 73, 777-784, 1968.

Energy, Mines and Resources Canada. Earth Physics Branch. Canadian Earthquakes-1978, by R.B. Horner, A.E. Stevens and R.J. Wetmiller, Seismological Series, 83, 1979.

\_\_\_\_\_. Canadian Earthquakes-1980, by R.J. Wetmiller, R.B. Horner, A.E. Stevens and G.C. Rogers, Seismological Series, 87, 1980.

\_\_\_\_\_. Canadian Earthquakes-1979, by R.J. Wetmiller, A.E. Stevens, and R.B. Horner, Seismological Series, 85, 1981.

\_\_\_\_\_. Canadian Earthquakes-1981, by J.A. Drysdale, R.J. Wetmiller, R.B. Horner, A.E. Stevens and

G.C.Rogers, Seismological Series, 90, 1984.

Burridge, R. and L. Knoppoff, "Body force equivalents for seismic dislocations", Bulletin of the Seismological Society of America, 54, 501, 1964.

Haskell, N.A., "Radiation pattern of Rayleigh waves from a fault of arbitrary dip and direction of motion in a homogeneous medium", Bulletin of the Seismological Society of America, 53, 619, 1963.

Kanamori, H. and D.L. Anderson, "Theoretical basis of some empirical relations in seismology", Bulletin of the Seismological Society of America, 65, 1073-1095, 1975.

Maruyama, T., "On the force equivalent of dynamic elastic dislocations with reference to the earthquake mechanism", Bulletin of Earthquake Research Institute Tokyo University, 41, 467, 1963.

Peltier, W.R. and J.T. Andrews, "Glacial-isostatic adjustment-I: The forward problem", Geophysical Journal of the Royal Astronomical Society, 46, 605-646, 1976.

Quinlan, G., "Postglacial rebound and the focal mechanisms of eastern Canadian earthquakes", Canadian Journal of Earth Sciences, 121, 1018-1023, 1984.

Stein, S., N.H. Sleep, R.J. Geller, S.-C. Wang and  
G.C. Kroeger, "Earthquakes along the passive margin of  
eastern Canada", Geophysical Research  
Letters, 6, 537-540, 1979.

Wu, P. and W.R. Peltier, "Viscous gravitational  
relaxation", Geophysical Journal of the Royal  
Astronomical Society, 70, 435-486, 1982.

APPENDIX 1

Green's function variations with time and distance

<u>r(km)</u>	<u>16000</u>	<u>13000</u>	<u>11000</u>	<u>9000</u>	<u>7000</u>
0	$1.0 \times 10^{-27}$	$5.2 \times 10^{-28}$	$3.7 \times 10^{-28}$	$2.7 \times 10^{-28}$	$2.1 \times 10^{-28}$
100	$7.2 \times 10^{-28}$	$4.2 \times 10^{-28}$	$3.1 \times 10^{-28}$	$2.3 \times 10^{-28}$	$1.7 \times 10^{-28}$
200	$2.9 \times 10^{-28}$	$2.1 \times 10^{-28}$	$1.7 \times 10^{-28}$	$1.3 \times 10^{-28}$	$1.0 \times 10^{-28}$
300	$1.1 \times 10^{-28}$	$6.4 \times 10^{-29}$	$5.0 \times 10^{-29}$	$4.0 \times 10^{-29}$	$3.2 \times 10^{-29}$
400	$6.6 \times 10^{-29}$	$8.3 \times 10^{-30}$	$2.6 \times 10^{-30}$	$6.4 \times 10^{-30}$	$7.3 \times 10^{-30}$
500	$4.3 \times 10^{-29}$	$2.1 \times 10^{-30}$	$1.3 \times 10^{-29}$	$1.7 \times 10^{-29}$	$1.8 \times 10^{-29}$
600	$2.8 \times 10^{-29}$	$4.6 \times 10^{-30}$	$1.2 \times 10^{-29}$	$1.4 \times 10^{-29}$	$1.5 \times 10^{-29}$
700	$1.9 \times 10^{-29}$	$6.4 \times 10^{-30}$	$9.9 \times 10^{-30}$	$1.1 \times 10^{-29}$	$1.0 \times 10^{-29}$
800	$1.2 \times 10^{-29}$	$7.1 \times 10^{-30}$	$8.8 \times 10^{-30}$	$8.3 \times 10^{-30}$	$7.0 \times 10^{-30}$
900	$7.8 \times 10^{-30}$	$7.2 \times 10^{-30}$	$7.7 \times 10^{-30}$	$6.7 \times 10^{-30}$	$5.2 \times 10^{-30}$
1000	$4.8 \times 10^{-30}$	$6.8 \times 10^{-30}$	$6.6 \times 10^{-30}$	$5.3 \times 10^{-30}$	$3.9 \times 10^{-30}$
1100	$2.6 \times 10^{-30}$	$6.3 \times 10^{-30}$	$5.6 \times 10^{-30}$	$4.2 \times 10^{-30}$	$2.9 \times 10^{-30}$
1200	$9.8 \times 10^{-31}$	$5.8 \times 10^{-30}$	$4.7 \times 10^{-30}$	$3.3 \times 10^{-30}$	$2.1 \times 10^{-30}$
1300	$-1.8 \times 10^{-31}$	$5.2 \times 10^{-30}$	$4.0 \times 10^{-30}$	$2.6 \times 10^{-30}$	$1.5 \times 10^{-30}$
1400M	$-1.0 \times 10^{-30}$	$4.7 \times 10^{-30}$	$3.3 \times 10^{-30}$	$2.0 \times 10^{-30}$	$1.1 \times 10^{-30}$
1500	$-1.6 \times 10^{-30}$	$4.2 \times 10^{-30}$	$2.8 \times 10^{-30}$	$1.6 \times 10^{-30}$	$7.4 \times 10^{-31}$
1600	$-2.1 \times 10^{-30}$	$3.7 \times 10^{-30}$	$2.3 \times 10^{-30}$	$1.2 \times 10^{-30}$	$4.9 \times 10^{-31}$
1700	$-2.4 \times 10^{-30}$	$3.3 \times 10^{-30}$	$1.9 \times 10^{-30}$	$9.0 \times 10^{-31}$	$3.1 \times 10^{-31}$
1800	$-2.6 \times 10^{-30}$	$2.9 \times 10^{-30}$	$1.6 \times 10^{-30}$	$6.7 \times 10^{-31}$	$1.7 \times 10^{-31}$
1900	$-2.7 \times 10^{-30}$	$2.6 \times 10^{-30}$	$1.3 \times 10^{-30}$	$4.8 \times 10^{-31}$	$7.4 \times 10^{-32}$
2000	$-2.8 \times 10^{-30}$	$2.2 \times 10^{-30}$	$1.0 \times 10^{-30}$	$3.4 \times 10^{-31}$	$3.9 \times 10^{-33}$



APPENDIX 2

Laurentide Ice load history(Peltier&Andrews,1976)

<u>Lat</u>	<u>E-lon</u>	<u>18</u>	<u>14</u>	<u>12</u>	<u>10</u>	<u>8</u>	<u>6</u>
80	265	500	300	200	200	0	0
80	270	1000	850	800	800	900	500
80	275	2000	1250	1200	1200	500	0
80	280	2000	1250	1200	1200	1000	0
80	285	1000	650	600	600	200	500
80	295	500	0	0	0	100	0
80	300	1000	1000	500	500	900	500
80	305	1500	1450	1200	1200	1450	1000
80	310	1500	1450	1200	1200	1450	1400
80	315	2000	2000	1950	1950	1950	2000
80	320	2200	2150	2100	2050	2000	1900
80	325	2500	2450	2400	2350	2250	2150
80	330	2200	2150	2050	2000	1800	1600
80	335	1500	1400	1300	500	0	0
75	250	200	300	300	0	0	0
75	255	200	1000	1000	0	0	0
75	260	1000	1400	1400	0	0	0
75	265	1000	1500	1500	600	0	0
75	270	1000	1200	1200	900	700	0
75	280	0	200	100	100	0	0
75	305	1000	900	600	500	900	500
75	310	2000	2000	2000	1950	1900	1900

75	315	2700	2700	2700	2650	2650	2700
75	320	2800	2750	2700	2650	2600	2500
75	325	3000	2950	2900	2850	2800	2700
75	330	3000	2950	2900	2850	2800	2700
75	335	2000	1950	1900	1800	1500	1300
70	235	10	300	300	0	0	0
70	240	1200	1400	1400	0	0	0
70	245	1800	1400	1400	0	0	0
70	250	1900	1600	1600	300	0	0
70	255	2100	2000	2000	1000	0	0
70	260	2200	2100	2100	1100	0	0
70	265	2200	2100	2100	1200	0	0
70	275	1900	1900	1900	1200	300	0
70	280	1600	1800	1800	1900	1400	0
70	285	1200	1100	1100	900	800	500
70	290	600	800	800	700	400	10
70	305	400	400	0	0	0	0
70	310	2000	2000	800	800	1000	200
70	315	2600	2600	2700	2650	2500	2000
70	320	3200	3150	3100	3050	3000	3000
70	330	2000	1950	1900	1600	1200	300
70	335	200	100	0	0	0	0
65	230	1000	500	300	0	0	0
65	235	1200	1550	1500	0	0	0
65	240	1800	1850	1800	0	0	0
65	245	2100	2000	2000	50	0	0
65	250	2300	2500	2400	1200	0	0
65	255	2600	2800	2800	1800	0	0

65	260	2600	3100	3100	2400	1000	500
65	265	2800	2800	2800	2800	1000	0
65	270	3000	2700	2700	2400	1000	0
65	275	2800	2700	2650	2000	600	0
65	280	2500	2350	2200	2400	1000	0
65	285	1950	2050	2050	1800	1200	0
65	290	1000	1500	1500	1100	1000	300
65	310	1800	1800	1000	1000	1000	500
65	315	2700	2700	2650	2650	2600	2600
60	225	1000	900	0	0	0	0
60	230	1000	900	800	0	0	0
60	235	1000	900	0	0	0	0
60	240	1200	1400	1300	0	0	0
60	245	2000	1850	1800	0	0	0
60	250	2400	2200	2000	0	0	0
60	255	2500	2400	2300	1100	400	0
60	260	2800	3050	2600	2100	1500	0
60	265	3200	3400	2900	2100	1200	0
60	270	3500	3400	3000	2050	600	0
60	275	3400	2800	2500	1800	400	0
60	280	3100	2400	2400	1600	400	0
60	285	2600	2050	2100	1400	600	0
60	290	1800	1500	1600	1300	600	0
60	295	500	800	600	700	300	0
60	315	200	100	0	0	0	0
55	230	1500	1400	1000	500	0	0
55	235	1500	1400	1000	0	0	0
55	240	1000	1000	0	0	0	0

55	245	1600	1000	200	0	0	0
55	250	2000	1800	1000	0	0	0
55	255	2000	2200	1100	0	0	0
55	260	2000	2400	1400	800	200	0
55	265	2400	2800	1900	1600	1200	0
55	270	2800	3050	200	2000	900	0
55	275	3000	3400	2800	2100	700	0
55	280	3500	3400	3250	2100	600	0
55	285	3000	3100	3000	2800	800	0
55	290	2000	2200	2500	3000	2000	500
55	295	1400	1400	1750	1600	140	0
55	300	600	600	600	0	0	0
50	235	1500	1300	0	0	0	0
50	240	1500	1000	1000	0	0	0
50	245	1000	800	0	0	0	0
50	250	800	0	0	0	0	0
50	255	900	300	0	0	0	0
50	260	1400	1200	0	0	0	0
50	265	1800	1900	0	0	0	0
50	270	2000	2200	900	300	0	0
50	275	2400	2700	1600	900	0	0
50	280	2800	2850	1850	1300	300	0
50	285	2800	2850	2100	1200	0	0
50	290	2600	2050	900	700	0	0
50	295	1800	1500	0	0	0	0
50	300	1700	1300	0	0	0	0
50	305	0	600	0	0	0	0
45	265	1200	1000	330	0	0	0

45	270	0	200	0	0	0	0
45	275	1900	900	200	0	0	0
45	280	1900	1400	900	0	0	0
45	285	1900	1400	200	0	0	0
45	290	1700	1200	800	0	0	0
45	295	1200	900	0	0	0	0
40	275	300	0	0	0	0	0
40	280	300	0	0	0	0	0

APPENDIX 3

theoretical seismic moment densities

<u>lat</u>	<u>E-lon</u>	<u>moment density</u>
40	220	590435
45	220	2102715
50	220	11686802
55	220	47826687
60	220	82566459
65	220	117771159
70	220	148654858
75	220	222267331
80	220	361845993
40	225	966362
45	225	2767068
50	225	12894640
55	225	50440071
60	225	32291766
65	225	29145892
70	225	17034900
75	225	9787915
80	225	25413015
40	230	1751402
45	230	5213506
50	230	22860052
55	230	53381848

60	230	34100935
65	230	20130510
70	230	39327813
75	230	10151105
80	230	27016772
40	235	2755662
45	235	8781596
50	235	28643092
55	235	34950091
60	235	9693244
65	235	16424263
70	235	36055313
75	235	13624743
80	235	25272363
40	240	3519537
45	240	11015292
50	240	26951516
55	240	33552563
60	240	19007651
65	240	5720164
70	240	19856715
75	240	22508236
80	240	34364805
40	245	3120163
45	245	5492293
50	245	18919333
55	245	21277414
60	245	6891155

65	245	21310349
70	245	16530541
75	245	39074261
80	245	43346857
40	250	3083466
45	250	2522805
50	250	18931457
55	250	9226801
60	250	21147508
65	250	24325154
70	250	25662064
75	250	43735064
80	250	49608938
40	255	4415533
45	255	2880377
50	255	9742957
55	255	25251562
60	255	22720195
65	255	22589542
70	255	40589690
75	255	21273163
80	255	50244803
40	260	7266309
45	260	20968809
50	260	11498867
55	260	84763540
60	260	42997353
65	260	40927508



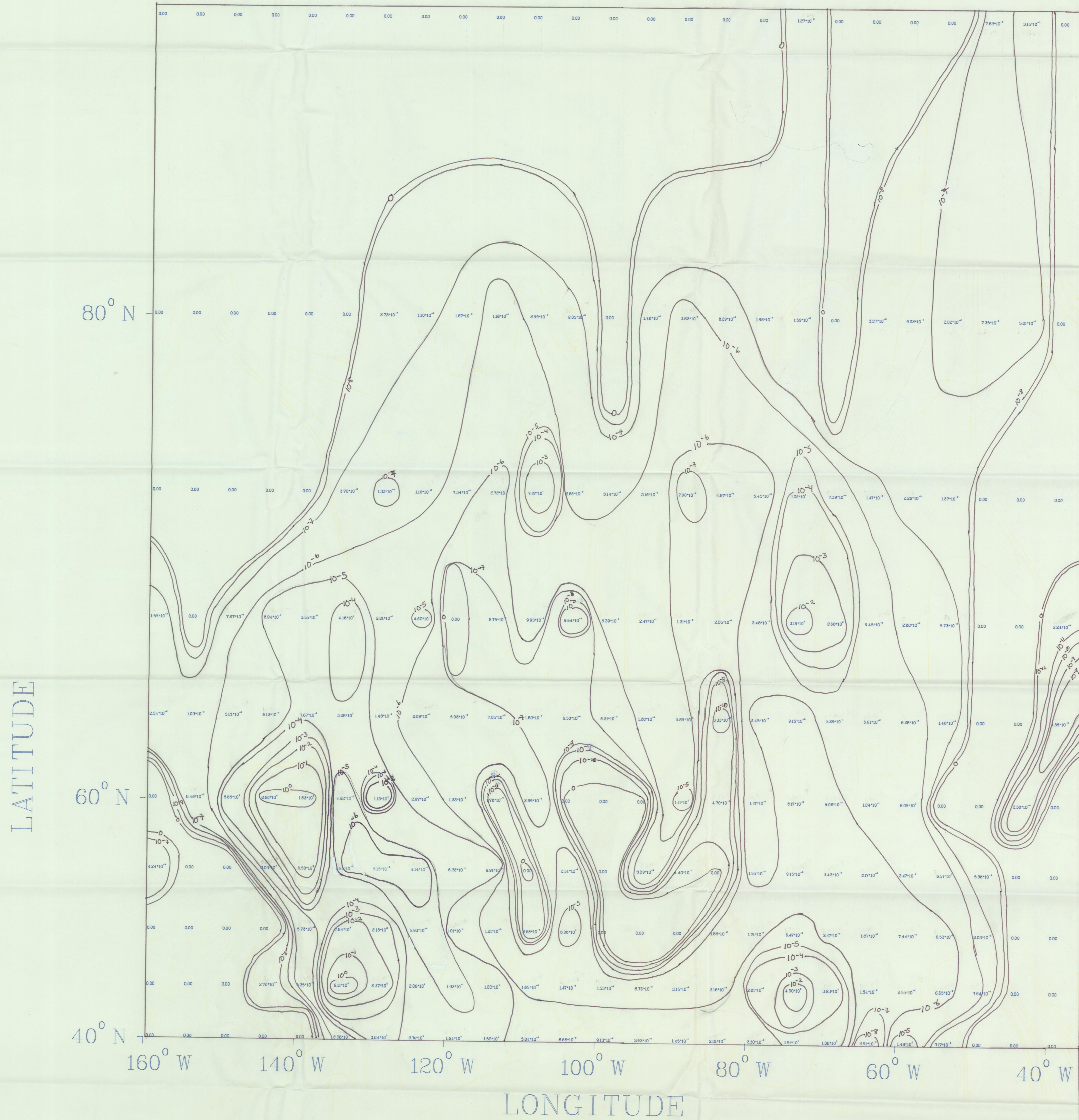
70	260	65088801
75	260	33857842
80	260	39075605
40	265	12305558
45	265	37787174
50	265	34962315
55	265	136692357
60	265	18219496
65	265	29113227
70	265	23974137
75	265	51830529
80	265	32402660
40	270	17950482
45	270	49911010
50	270	26724777
55	270	79416721
60	270	38640953
65	270	34039621
70	270	100172131
75	270	51323412
80	270	33707459
40	275	6433154
45	275	24734738
50	275	7829172
55	275	33629035
60	275	13462310
65	275	20741250
70	275	37007348

75	275	41074894
80	275	79637657
40	280	11014620
45	280	20452942
50	280	14348787
55	280	12535910
60	280	6417234
65	280	56720108
70	280	92349726
75	280	26622310
80	280	101484263
40	285	7646644
45	285	15728513
50	285	36667316
55	285	36083873
60	285	34828490
65	285	67021891
70	285	14282757
75	285	37876009
80	285	82948042
40	290	8693150
45	290	18700683
50	290	27047921
55	290	31905341
60	290	33363058
65	290	39844265
70	290	41672642
75	290	44219673

80	290	31931129
40	295	8290114
45	295	16168913
50	295	22495431
55	295	19018268
60	295	29740286
65	295	71802877
70	295	55272354
75	295	36219820
80	295	25111161
40	300	13168296
45	300	19169619
50	300	19009941
55	300	25299617
60	300	44621818
65	300	78849457
70	300	82868880
75	300	14294706
80	300	46021793
40	305	11579760
45	305	11382241
50	305	19366294
55	305	27616257
60	305	26606517
65	305	21480096
70	305	41766033
75	305	24340242
80	305	50121253

40	310	4780103
45	310	15919407
50	310	47700356
55	310	78965697
60	310	65663959
65	310	154252177
70	310	228867680
75	310	280748629
80	310	511334123

# SEISMIC MOMENT DENSITY



OBSERVED SEISMICITY  
OF CANADA  
(N·m/m<sup>2</sup>·yr)  
Mercator Projection

A.L.BENT 1985

17.14.04.

85/02/07.

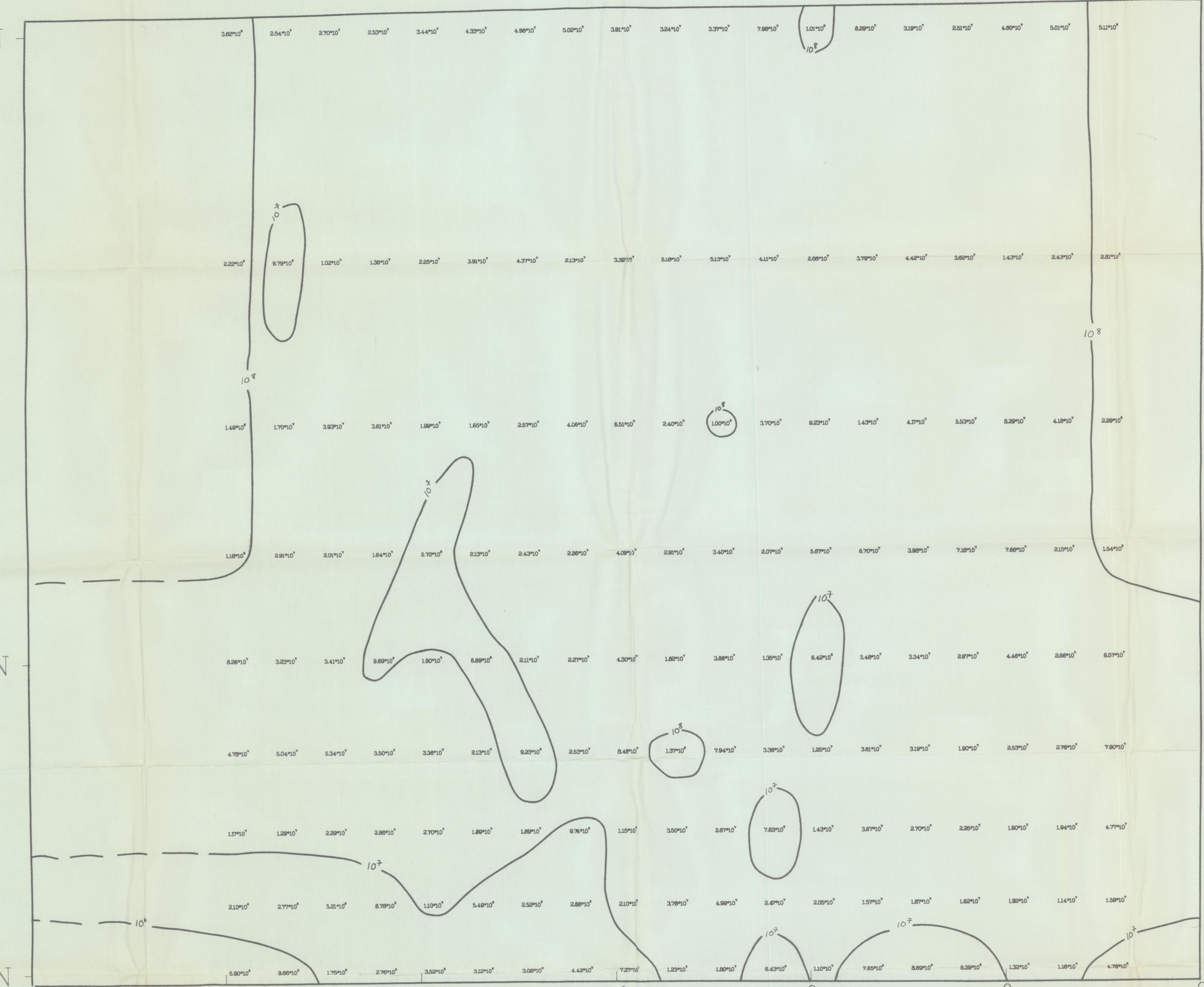
JN=ALYY:: IAR2801

LAT

80° N

60° N

40° N



160° W

140° W

120° W

100° W

80° W

60° W

40° W

LON

THEORETICAL SEISMICITY  
OF CANADA

(N·m/m<sup>2</sup>·yr)

Mercator Projection

A.L. Bent

1985